This article has been accepted for publication in a future issue of this journal, but has not been fully edited. Content may change prior to final publication. Citation information: DOI 10.1109/TVT.2014.2298395, IEEE Transactions on Vehicular Technology

Performance of p-norm Detector in AWGN, Fading and Diversity Reception

Vesh Raj Sharma Banjade, Chintha Tellambura, *Fellow, IEEE* and Hai Jiang, *Member, IEEE*

***Abstract*—Performance analysis of the p-norm detector to date has been limited to ad hoc approximations, non-fading channels and Rayleigh fading. To overcome these limitations, we develop several analytical/numerical solutions for the detection probability P_d and the false alarm probability P_f, which are necessary to specify the receiver operating characteristic curves of the p-norm detector. First, for non-fading channels (additive white Gaussian noise only), the moment generating function (MGF) of the decision variable is derived in two forms: (i) closed-form for even-integer p and (ii) series-form for arbitrary p. To evaluate P_d and P_f, a numerical method utilizing the Talbot inversion is developed for case (i), and an infinite series expansion with convergence acceleration based on the ϵ-algorithm is derived for case (ii). As an alternative to MGF-based analysis, a Laguerre polynomial series is also used to derive new P_d and P_f approximations. Second, series-form MGF-based P_d expressions are derived for κ-μ and α-μ fading channels. Third, for antenna diversity reception, new p-law combining (pLC) and p-law selection (pLS) schemes are proposed. The performance of these combiners with the p-norm detector is derived for Nakagami-m fading and is compared to that of the classical maximal ratio combining (MRC) and selection combining (SC). Interestingly, both pLC and pLS perform similarly to SC at low signal-to-noise ratio (SNR) but outperform it at relatively high SNR, with pLC performing closer to the optimal MRC. Numerical results are presented to verify the derived results and to provide further insights.**

***Index Terms*—p-norm detector, energy detector, detection probability, false alarm probability, moment generating function, diversity combining.**

I. Introduction

WIRELESS signal detection is essential for applications such as radar [1], spectrum sensing in cognitive radios (CRs) [2], and impulse radio-based ultra-wideband (UWB) communications [3]. Three most popular signal detection techniques are matched filter detector, energy detector, and cyclostationarity-based detector [2]. Matched filtering is a coherent detection technique requiring demodulation of the signal under test (SUT) and thus needs *a priori* information about the SUT (e.g., modulation format, pulse shaping, phase, etc.). However, in practice, such information may not always be available at the receiver thus rendering the matched filter detector infeasible. The cyclostationarity-based detector exploits the built-in periodicity (if any) in the modulated signal resulting due to sine wave carriers, pulse trains or cyclic prefixes [2]. Thus, while periodicity may be used to distinguish a modulated signal from noise, identification of periodicity requires a large sampling rate and high computational complexity. Moreover, such technique is highly sensitive to the sampling clock errors [4]. These facts motivate the use of non-coherent detectors like the energy detector (ED) [5] which operates without any *a priori* SUT information and has a low implementation complexity. Recently, the decision variable of ED was generalized as

$$T = \frac{1}{N}\sum_{i=1}^{N} |y_i|^p, \tag{1}$$

where y_i $\forall i \in \{1, 2, ..., N\}$ is the i-th received signal sample, $p > 0$ is an arbitrary constant, and N is the total number of samples [6], [7]. This detector, also known as the improved energy detector [6], [8], [9] or the L_p-norm detector [7], is referred to as the *p-norm detector* throughout this work. Clearly, ED, whose performance has been analyzed extensively [10]–[17], is a special case of the p-norm detector (i.e. $p = 2$).

Recent results indicate the advantages of the p-norm detector compared to ED. First, choosing $p \neq 2$ may yield a performance gain and hence the best p value depends upon the probability of correct detection, the probability of false alarm, the signal-to-noise ratio (SNR), and the received signal sample size [6]. Second, adaptive optimization of p yields remarkable performance gain over the ED with the resulting performance closer (than ED) to the locally optimal detector[1] at very low SNRs [7]. Moreover, the optimal p that minimizes the total error rate is not equal to 2 in general, and other p values may provide more reliable (less erroneous) detection performance [8], [9].

However, the existing p-norm detector performance analyses are limited by some ad hoc assumptions. For example, reference [6] assumes T as Gamma distributed, an approximation that is more accurate for lower p, higher N and relatively low SNR. For CR networks operating at low SNRs, reference [7] assumes a large N ($N \gg 1$) such that the central-limit theorem (CLT) holds, and thus T is approximately Gaussian. However, in practice, the requirement of a low sensing time conflicts with the large sample assumption. The assumption of a single received signal sample ($N = 1$) per CR and per antenna used in [8] and [9] severely limits the reliability of detection. Overall, what is lacking is a more exact and general performance analysis of the p-norm detector.

Manuscript received July 20, 2013; revised November 25, 2013; accepted December 22, 2013. The associate editor coordinating the review of this paper and approving it for publication was Dr. M. Yacoub. This work was supported by the Natural Science and Engineering Research Council (NSERC) of Canada. The authors are with the Department of Electrical and Computer Engineering, University of Alberta, Edmonton, AB, Canada T6G 2V4. (e-mail: {sharmaba,hai1}@ualberta.ca, chintha@ece.ualberta.ca).

[1]A locally optimal detector is asymptotically optimal at low SNR.

This article has been accepted for publication in a future issue of this journal, but has not been fully edited. Content may change prior to final publication. Citation information: DOI 10.1109/TVT.2014.2298395, IEEE Transactions on Vehicular Technology

Moreover, the existing analyses are limited to additive white Gaussian noise (AWGN) (non-fading) [6] and Rayleigh-fading [7], [8], [9]. However, spatially correlated non-homogeneous scattering occurs in real propagation environments [18], which are better modeled by the κ-μ and the α-μ distributions. The κ-μ distribution is a small-scale fading model with line-of-sight (LOS) conditions (indicated by κ) and μ is associated with the number of multipath clusters [18]. The κ-μ model includes the Rayleigh, Rician and Nakagami-m fading models as special cases. On the other hand, the α-μ fading model relates α and μ to the non-linearity and to the number of multipath components, respectively [19]. Likewise, the α-μ model includes Weibull, Gamma, Nakagami-m, Rayleigh, exponential and one-sided Gaussian models as special cases. Moreover, field trials have confirmed that the κ-μ and the α-μ distributions outperform the classical fading models in fitting the experimental data due to the comprehensive range (versatility) of these models' parameter values [18], [19]. Thus, evaluation of the p-norm detection performance in these generalized fading models is useful

(i) to quantify the performance loss (relative to the non-fading case) incurred in realistic fading channels and, potentially, to help in designing detectors robust to such impacts, and
(ii) to determine the required SNR and related parameter values necessary to achieve a prescribed performance in non-homogeneous and non-linear propagation environments.

In addition, as wireless fading fundamentally limits performance, antenna diversity-combining techniques are used to mitigate its impact [20]. Thus, achievable performance gains by integrating these techniques with the p-norm detector must be quantified. Hence, the p-norm detection performance analysis in generalized fading channels and with diversity reception is of interest.

Such analysis is challenging because the distribution of T in (1) appears intractable (in general). This distribution is necessary to obtain the detection probability (P_d) and the false alarm probability (P_f), which are essential to specify the receiver operating characteristic (ROC) curves of the detector (see Section V). Since the exact probability density function (PDF)-based analysis appears intractable, we consider utilizing the moment generating function (MGF) of T. Fortunately, the MGF of T can be obtained as a product of MGFs of its summands (for statistically independent summands) and thus is more amenable to a tractable analysis. Furthermore, we show that this approach facilitates analysis in fading and diversity reception. To the best of our knowledge, no such comprehensive p-norm detection performance analysis is currently available. This paper addresses the aforementioned issues in the following ways:

- First, for non-fading channels (i.e. channels with AWGN only), three solutions for P_d and P_f are developed: (i) for even-integer values of p, a closed-form MGF of the decision variable T is derived. Then, by using the Talbot's method for Laplace transform inversion [21], which is highly accurate and easy to program [22], a computationally efficient solution is developed; (ii) for any arbitrary p, series-based MGF of T is derived and utilized to obtain accurate infinite series expressions with convergence acceleration based on the ϵ-algorithm [23]; (iii) a generalized Laguerre polynomial series [24] for the distribution of T is used to derive new approximate expressions. This approximation is more versatile than the Gamma approximation [6] and more accurate than the CLT approximation (for a few samples).[2]
- Second, to characterize the p-norm detector performance across a wide range of realistic multipath fading environments, the series MGF-based analysis is extended to obtain accurate series-form expressions for the average[3] probability of detection over κ-μ and α-μ fading.
- Third, to assess the performance with antenna diversity reception (in fading), two non-coherent combining schemes, p-law combining (pLC) and p-law selection (pLS), are proposed. These combiners are compared against two classical diversity-combining techniques, maximal ratio combining (MRC) and selection combining (SC), by deriving their performance in Nakagami-m fading channels. Interestingly, both pLC and pLS perform similarly to the traditional SC at low SNR but outperform it at relatively high SNR, with pLC performing closer to the optimal MRC. Furthermore, since pLC and pLS do not require any channel state information (CSI), they are more useful than classical MRC and SC schemes for the p-norm detector (which functions without any CSI).

The organization of this paper is as follows. The system model is described in Section II. The detection and false alarm probabilities in the AWGN channel are derived in Section III. The series MGF-based analysis is utilized to derive the average detection probabilities over κ-μ and α-μ fading and with antenna diversity reception over Nakagami-m fading in Section IV. Numerical results are discussed in Section V. Concluding remarks are made in Section VI.

II. System Model

Notations $\mathcal{CN}(\overline{x}, \sigma_x^2)$, $\mathbb{P}(\cdot)$, $u(\cdot)$, $\mathbb{E}[\cdot]$, Var$[\cdot]$, $\Re\{\cdot\}$, $\jmath$ and $\mathcal{L}^{-1}[\cdot]$, respectively, denote complex Gaussian distribution with mean $\overline{x}$ and variance σ_x^2, probability of an event, unit step function, mathematical expectation, variance, real part of a complex quantity, imaginary unit ($\sqrt{-1}$), and inverse Laplace transform.

The problem of signal detection can be formulated as a binary hypothesis test where hypotheses H_0 and H_1 represent the cases when the SUT is absent and present, respectively. After baseband down conversion and a sampling process, the i-th signal sample $\forall i \in \{1, 2, ..., N\}$ can be written as

$$y_i = \begin{cases} w_i & : H_0, \\ h_i S_i + w_i & : H_1, \end{cases}$$

where h_i, S_i and w_i are i-th sample of the complex fading channel gain, SUT and noise, respectively. The signal and

[2]The CLT approximation is a reference benchmark. It is considered for p-norm detection in [7] and in general, for signal detection, in [25].

[3]The term "average" implies the mathematical expectation with respect to the multipath fading distribution.

This article has been accepted for publication in a future issue of this journal, but has not been fully edited. Content may change prior to final publication. Citation information: DOI 10.1109/TVT.2014.2298395, IEEE Transactions on Vehicular Technology

the noise samples are independent and identically distributed (i.i.d.) with $S_i \sim \mathcal{CN}(0, \sigma_S^2)$ [4] and $w_i \sim \mathcal{CN}(0, \sigma_w^2)$. The channel samples are i.i.d as well.[5] The signal, noise and the channel gain are statistically independent of each other.

In a recent study [6], it is argued that the ED, which is based on the maximization of the likelihood function, does not necessarily maximize the probability of correct detection or minimize the probability of erroneous decision. This fact has led to the introduction of the p-norm detector [6], [7]. After normalizing the decision variable in (1), the p-norm decision rule may be written as

$$T = \frac{1}{N}\sum_{i=1}^{N} Y_i^p \underset{H_0}{\overset{H_1}{\gtrless}} \lambda, \tag{2}$$

where we define $Y_i \triangleq |y_i|/\sigma_w$ and λ is the detection threshold. Under the system model considered, the distribution of the i-th received signal sample under H_0 and H_1 follows complex Gaussian distribution with $y_i|H_0 \sim \mathcal{CN}(0, \sigma_w^2)$ and $y_i|H_1 \sim \mathcal{CN}(0, \sigma_w^2(1+\gamma_i))$, respectively, with $\gamma_i \triangleq |h_i|^2\sigma_S^2/\sigma_w^2$ being the instantaneous received SNR of the i-th sample.

Two important performance metrics of the detector are the detection probability P_d, and the false alarm probability P_f, which are defined as

$$\begin{aligned} P_d &\triangleq \mathbb{P}(T > \lambda | H_1) = 1 - F_{T|H_1}(\lambda), \\ P_f &\triangleq \mathbb{P}(T > \lambda | H_0) = 1 - F_{T|H_0}(\lambda). \end{aligned} \tag{3}$$

Here P_d and P_f are the complementary cumulative distribution functions (CCDFs) of T under hypothesis $H \in \{H_1, H_0\}$, respectively, with $F_{T|H}(\cdot)$ denoting the CDF under hypothesis H. The baseline objective of this work is to develop expressions for both P_d and P_f. Note that P_d depends on the received SNR whereas P_f does not. Thus, in the fading channels, only the detection probability needs to be averaged over the PDF of the received SNR.

III. Derivation of P_d and P_f in AWGN

In AWGN, $h_i = 1, \forall i \in \{1, 2, ..., N\}$ and thus we define $\gamma \triangleq \sigma_S^2/\sigma_w^2$ dropping the subscript 'i'. The results for AWGN derived in this section establish an upper bound on the achievable detection performance and also facilitate the subsequent extension to multipath fading and diversity reception scenarios. Moreover, these results are important for a fair comparison with the existing Gamma approximation [6].

As the distribution of y_i under each hypothesis is complex Gaussian, the squared amplitude of normalized i-th sample Y_i^2 is exponentially distributed as $Y_i^2|H_0 \sim e^{-x}u(x)$ for H_0, and $Y_i^2|H_1 \sim [1/(1+\gamma)]e^{-x/(1+\gamma)}u(x)$ for H_1. The MGF of the detector's decision variable T under hypothesis H is defined as $\mathcal{M}_{T|H}(s) \triangleq \mathbb{E}_{T|H}\left[e^{-sT}\right]$. Since the noise samples as well as the signal samples are i.i.d. and mutually independent of each other, the MGF of T can be expressed as a product of the MGFs of Y_i^p/N $\forall i \in \{1, 2, ..., N\}$, given as

$$\begin{aligned} \mathcal{M}_{T|H}(s) &= \left[\ \mathbb{E}_{T|H}\left(e^{-\frac{s}{N}\left(\frac{|y_i|}{\sigma_w}\right)^{2\cdot\frac{p}{2}}}\right)\ \right]^N \\ &= \left[\ \int_0^\infty e^{-\frac{s}{N}x^{p/2}} \cdot A_H e^{-A_H x} dx\ \right]^N, \end{aligned} \tag{4}$$

where A_H is a parameter under hypothesis H defined as

$$A_H \triangleq \begin{cases} 1 & H_0, \\ 1/(1+\gamma) & H_1. \end{cases}$$

A. Closed-form MGF-based analysis for even-integer p

Considering even-integer p and using [31, eq. (4)] to solve the integral in (4) results in a closed-form MGF of the form

$$\mathcal{M}_{T|H}(s) = \left[\frac{\sqrt{p/2}}{(\sqrt{2\pi})^{p/2-1}} G_{1,\frac{p}{2}}^{\frac{p}{2},1}\left(\frac{2^{p/2}A_H^{p/2}N}{p^{p/2}s}\middle|\begin{matrix}1\\ \frac{2}{p}, \frac{4}{p}, ..., 1\end{matrix}\right)\right]^N, \tag{5}$$

where $G_{\cdot,\cdot}^{\cdot,\cdot}(\cdot)$ is the Meijer's G-function [32, eq. (4)]. Then, the CDF of T under H, $F_{T|H}(\lambda)$, can be obtained from the inverse Laplace transform of $\mathcal{M}_{T|H}(s)/s$ as

$$\begin{aligned} F_{T|H}(\lambda) &= \frac{1}{2\pi\jmath}\int_B \frac{\mathcal{M}_{T|H}(s)}{s}\, e^{s\lambda} ds \\ &= \frac{1}{2\pi\jmath}\int_B \widehat{\mathcal{M}}_{T|H}(s)\, e^{s\lambda} ds, \end{aligned} \tag{6}$$

where B is the Bromwich contour [21] and we define $\widehat{\mathcal{M}}_{T|H}(s) = \mathcal{M}_{T|H}(s)/s$. An analytical expression for $F_{T|H}(\lambda)$ appears intractable. Moreover, a direct computation of the above integral over B is impractical due to possible oscillations of $e^{s\lambda}$ (where $s = c + \jmath w$) as $|w| \to \infty$, and thus Talbot suggested a deformation of the contour [21] for evaluating such integrals. To improve the numerical stability of such evaluation in a fixed-precision computing environment, a multi-precision method termed the "fixed Talbot method" was proposed in [22], which suggests an alternative form of the integral as

$$F_{T|H}(\lambda) = \frac{1}{2\pi\jmath}\int_{-\pi}^{\pi} \widehat{\mathcal{M}}_{T|H}[s(\theta)] \cdot s'(\theta) e^{\lambda s(\theta)} d\theta, \tag{7}$$

where $s(\theta) = r\theta(\cot\theta + \jmath)$ with $|\theta| < \pi$, $s'(\theta)$ being the derivative of $s(\theta)$ w.r.t. θ, and $r = 2\mathcal{W}/(5\lambda)$ with integer $\mathcal{W}$ controlling the desired precision for the fixed Talbot method [22]. The integral in (7) can then be evaluated by using the trapezoidal rule with step size $\pi/\mathcal{W}$ and $\theta_k = k\pi/\mathcal{W}$, and hence the CDF $F_{T|H}(\lambda)$ can be computed as [22], [33]

$$\begin{aligned} F_{T|H}(\lambda) = \frac{r}{\mathcal{W}}\Bigg(&\frac{1}{2}\widehat{\mathcal{M}}_{T|H}(r)e^{r\lambda} \\ &+ \sum_{k=1}^{\mathcal{W}-1} \Re\{e^{\lambda s(\theta_k)}\widehat{\mathcal{M}}_{T|H}[s(\theta_k)]\,(1 + \jmath\sigma(\theta_k))\}\Bigg), \end{aligned} \tag{8}$$

[4] Gaussian signal assumption is valid, for example, in an Orthogonal Frequency Division Multiplexing (OFDM) signal having a large number of sub-carriers [26], [27]; in frequency-shift keying (FSK) signals that can be reasonably approximated as Gaussian process due to the complex time-structure; in radio-spectroscopy where the radiation process can be approximated as a Gaussian process due to collision-broadening or other atomic effects; or in radio-astronomy where the signals generated from radio-stars or gas clouds can be modeled as Gaussian which has varying intensities over the radio spectrum [28].

[5] This assumption is valid for time-selective fading channels, which are typical in some practical situations (e.g., when there is relative motion between the transceiver pair [29], or when the transceiver pair have a carrier frequency offset due to their oscillators' mismatch [30]). Nevertheless, the analytical approach developed in the paper can be readily extended for time-flat fading channels as well.

This article has been accepted for publication in a future issue of this journal, but has not been fully edited. Content may change prior to final publication. Citation information: DOI 10.1109/TVT.2014.2298395, IEEE Transactions on Vehicular Technology

where $\sigma(\theta) = \theta + (\theta\cot\theta - 1)\cot\theta$. Based on [22], the number of significant digits of $F_{T|H}(\lambda)$ calculated in (8) is approximately equal to $0.6\mathcal{W}$.

Then, the CCDF of $T|H$ can immediately be expressed as

$$\mathbb{P}(T \geq \lambda|H) = 1 - \frac{r}{\mathcal{W}}\left(\frac{1}{2}\widehat{\mathcal{M}}_{T|H}(r)e^{r\lambda} + \sum_{k=1}^{\mathcal{W}-1} \Re\{e^{\lambda s(\theta_k)}\widehat{\mathcal{M}}_{T|H}[s(\theta_k)]\,(1+\jmath\sigma(\theta_k))\}\right). \quad (9)$$

By substituting $A_H = 1/(1+\gamma)$ and $A_H = 1$, respectively, into (5) and subsequently using (9), P_d and P_f can be computed accurately. Note that a numerical software package such as MATHEMATICA can be readily used for the evaluation of (9). Hence, (9) offers a computationally attractive solution for both P_d and P_f when p is an even-integer.

B. Series MGF-based analysis for arbitrary p

In this section, starting from the derivation of a series-form MGF of T, novel series solutions are obtained for P_d and P_f which are valid for any arbitrary p. Substituting $e^{-x} = \sum_{v=0}^{\infty}(-1)^v x^v/v!$ inside the integral in (4), interchanging the order of integration and summation, and using [32, eq. (3.326.2)], we have

$$\mathcal{M}_{T|H}(s) = \left[\frac{2}{p}\sum_{v=0}^{\infty}\frac{(-1)^v A_H^{v+1}N^{2(v+1)/p}}{v!\;\; s^{2(v+1)/p}}\Gamma\left(\frac{2(v+1)}{p}\right)\right]^N, \quad (10)$$

where $\Gamma(x) = \int_0^\infty t^{x-1}e^{-t}dt$ is the Gamma function [34, eq. (6.1.1)]. By using [32, eq. (0.314)] to further simplify (10), the series-form MGF can be obtained as

$$\mathcal{M}_{T|H}(s) = \frac{2^N}{p^N}\sum_{v=0}^{\infty}\frac{C_{v|H}N^{2(v+N)/p}}{s^{2(v+N)/p}}, \quad (11)$$

where

$$C_{v|H} = \frac{1}{v\,\Gamma(2/p)A_H}\sum_{k=1}^{v}(kN - v + k)\frac{(-1)^k}{k!} \times \Gamma\left(\frac{2(k+1)}{p}\right)A_H^{k+1}\;\; C_{v-k|H},\;\; v \geq 1,$$

and $C_{0|H} = [\Gamma(2/p)A_H]^N$. The CDF $F_{T|H}(\lambda)$ can then be obtained by using the inverse Laplace transform

$$\mathcal{L}^{-1}\left[\frac{\Gamma(a+1)}{s^{a+1}}\right] = t^a,\;\; a > -1,$$

on $\mathcal{M}_{T|H}(s)/s$, and subsequently, the CCDF under hypothesis H can be expressed as

$$\mathbb{P}(T > \lambda|H) = 1 - \frac{2^N}{p^N}\sum_{v=0}^{\infty}\frac{C_{v|H}(N\lambda)^{2(v+N)/p}}{\Gamma\left(\frac{2(v+N)}{p}+1\right)}. \quad (12)$$

Thus, the use of (12) after substituting $A_H = 1/(1+\gamma)$ and $A_H = 1$ for hypothesis H_1 and H_0 in the expression for $C_{v|H}$ yields the detection probability P_d and the false alarm probability P_f, respectively. For the sake of brevity, we omit re-writing similar expressions.

TABLE I: The ϵ-table.

$c=-2$	$c=-1$	$c=0$	$c=1$	...
0	$\epsilon(0,0)=S_0$	$\epsilon(0,1)$	$\epsilon(0,2)$	...
0	$\epsilon(1,0)=S_1$	$\epsilon(1,1)$	$\epsilon(1,2)$	...
$\vdots$	$\vdots$	$\vdots$	$\vdots$	$\iddots$
0	$\epsilon(\eta-3,0)=S_{\eta-3}$	$\epsilon(\eta-3,1)$	$\epsilon(\eta-3,2)$	
0	$\epsilon(\eta-2,0)=S_{\eta-2}$	$\epsilon(\eta-2,1)$		
0	$\epsilon(\eta-1,0)=S_{\eta-1}$			

Moreover, (12) can be expressed as an alternating series-sum such that the CCDF under hypothesis H is $\mathbb{P}(T > \lambda|H) = 1 - \sum_{v=0}^{\infty}(-1)^v D_{v|H}$, with

$$D_{v|H} \triangleq \frac{2^N}{p^N}\cdot\frac{|C_{v|H}|(N\lambda)^{2(v+N)/p}}{\Gamma\left(\frac{2(v+N)}{p}+1\right)}.$$

Our experiments show that $D_{v|H}$ is readily decreasing with increasing v. Thus, the infinite sum $\mathcal{S}_\infty = \sum_{k=0}^{\infty}(-1)^n D_{k|H}$ can be estimated by a partial sum of its n_t terms of the form $\mathcal{S}_{n_t} = \sum_{k=0}^{n_t}(-1)^n D_{k|H}$, and the truncation error E_{tr} can thus be upper-bounded as $|E_{tr}| < |D_{n_t+1|H}|$. Although the absolute truncation error $|E_{tr}|$ readily decreases with increasing n_t, the rate of convergence may be accelerated by using the powerful ϵ-algorithm. The ϵ-algorithm transforms the original series into convergents of its associated continued fractions thus resulting in a faster rate of convergence (i.e. fewer terms to achieve a given precision) [23].

The objective of the ϵ-algorithm is to estimate $\mathcal{S}_\infty$ by using as few partial sums as possible. This algorithm generates a two-dimensional triangular array called the ϵ-table as shown in Table I with entries $\epsilon(k, c+1)$, where $k = 0, 1, 2, ...$ is the row index and $c = -2, -1, 0, 1, 2, ...$ determines the column index. The first two columns (column '-2' and column '-1') are initialized as $\epsilon(k,-1) = 0$, $\epsilon(k,0) = \mathcal{S}_k\;\forall k \in \{0, 1, ..., \eta-1\}$, with η representing the total number of terms used in the partial sum. The remaining columns are updated as

$$\epsilon(k, c+1) = \epsilon(k+1, c-1) + [\epsilon(k+1, c) - \epsilon(k, c)]^{-1},$$

where $c \geq 0$. As the value of η is increased (which leads to the corresponding increase in the number of columns), the even columns of the ϵ-table contain increasingly accurate estimates of S_∞ [23]. The algorithm stops (no further increase in η) when the desired precision is attained at a particular even column (i.e., the values in the column converge with the desired precision). Then any value in the column can be used as an estimated $\mathcal{S}_\infty$ and the corresponding value of η represents the number of terms needed in the ϵ-algorithm. For example, for a 2.5-norm detector at SNR of 0 dB, with $N = 4$ at $P_f = 0.01$, $\eta = 21$ terms are sufficient for the ϵ-algorithm applied to (12) for computing P_d with 4-decimal points accuracy, as compared to $n_t = 33$ terms without convergence acceleration. More examples in Table II (obtained with accuracy of 4-decimal points) clearly show the advantage of the ϵ-algorithm in increasing the convergence rate (hence reducing the computation time).

This article has been accepted for publication in a future issue of this journal, but has not been fully edited. Content may change prior to final publication. Citation information: DOI 10.1109/TVT.2014.2298395, IEEE Transactions on Vehicular Technology

TABLE II: Number of terms needed in (12) for computation of P_d with and without (w.o.) using ϵ-algorithm.

	$\gamma=-15$ dB, $\lambda=5$						$\gamma=0$ dB, $\lambda=7$			$\gamma=10$ dB, $\lambda=7$			
p	1.8		2.5		3.5		1.8	2.5	3.5	1.5		4	
N	2	4	2	4	2	4	4	4	4	5	10	5	10
Eq. (12) w.o. ϵ-algorithm	41	79	25	47	19	33	59	33	23	29	59	7	7
ϵ-algorithm	21	63	15	23	13	19	27	19	13	15	33	5	3

C. Generalized Laguerre polynomial series-based approximation

In this section, we derive approximate expressions for the detection and false alarm probabilities based on a generalized Laguerre polynomial series representation of the decision variable.

We propose approximating the PDF of the decision variable T by a weighted sum of the generalized Laguerre polynomials of the form [24] [6]

$$f_T(z)\approx\frac{\beta z^{\alpha}e^{-z}}{\Gamma(\alpha+1)}\sum_{n=0}^{N_g} r_n L_n^{\alpha}(z),\quad z\geq 0,\quad \alpha\geq -1, \tag{13}$$

in which

$$L_n^{\alpha}(z)\triangleq\sum_{u=0}^{n}\frac{(-1)^u}{u!}\frac{\Gamma(\alpha+n+1)}{\Gamma(n-u+1)\Gamma(\alpha+u+1)}z^u$$

is the generalized Laguerre polynomial [38], and the coefficient r_n is given by[7]

$$r_n=\frac{n!\,\Gamma(\alpha+1)}{\beta\,\Gamma(n+\alpha+1)}\sum_{\nu=0}^{n}\frac{(-1)^{\nu}\,\Gamma(\alpha+n+1)\beta^{\nu}m_{\nu}}{\nu!\,\Gamma(n-\nu+1)\Gamma(\alpha+\nu+1)}, \tag{14}$$

where $m_{\nu}=\mathbb{E}(T^{\nu})$ is the ν-th moment of T, and the parameters α and β are given by

$$\alpha=\frac{2m_1^2-m_2}{m_2-m_1^2},\quad \beta=\frac{m_1}{m_2-m_1^2}.$$

Note that the moment m_{ν} depends on the hypothesis $H\in\{H_0,H_1\}$ and can be obtained by multinomial expansion of (2) followed by some algebra as

$$m_{\nu}|H=\frac{1}{N^{\nu}}\sum_{\mathbf{\Lambda}_{\nu}}\binom{\nu}{k_1,...,k_N}\mathbb{E}_{Y_1,Y_2,...,Y_N|H}\left[\prod_{i=1}^{N}Y_i^{k_ip}\right],$$

where $\mathbf{\Lambda}_{\nu}=[k_1,...,k_N|k_1+...+k_N=\nu,k_1,...,k_N\geq 0]$. Utilizing the i.i.d. property of $Y_i\ \forall i\in\{1,2,...,N\}$ followed by evaluation of the mathematical expectation, we can show that

$$m_{\nu}|H=\frac{1}{N^{\nu}}\sum_{\mathbf{\Lambda}_{\nu}}\binom{\nu}{k_1,...,k_N}\prod_{i=1}^{N}A_H^{-\frac{k_ip}{2}}\Gamma\left(\frac{k_ip}{2}+1\right). \tag{15}$$

By substituting the definition of $L_n^{\alpha}(z)$ into (13), integrating the resulting expression from $z=0$ to $z=\lambda$, and changing the order of integration and summation followed by some algebra, the CDF of T can be obtained as

$$F_T^{\text{Lag}}(\lambda)=\sum_{n=0}^{N_g}\frac{r_n\beta}{\Gamma(\alpha+1)}\sum_{u=0}^{n}\zeta(u,n,\alpha,\lambda), \tag{16}$$

in which

$$\zeta(u,n,\alpha,\lambda)\triangleq\frac{(-1)^u\Gamma(\alpha+n+1)}{u!\Gamma(n-u+1)\Gamma(\alpha+u+1)}\mathcal{G}(\alpha+u+1,\lambda),$$

and $\mathcal{G}(a,x)=\int_0^x e^{-t}t^{a-1}dt$ is the lower incomplete Gamma function [34, eq. (6.5.2)].[8] Since the moments m_i of T are different under the two hypotheses as revealed by (15), the parameters α, β and r_n are also hypothesis-dependent. Using (15) for each hypothesis $H\in\{H_0,H_1\}$ in the definition of α and β, we get

$$\begin{aligned}&\alpha|H_0=\alpha|H_1=\tfrac{(N+1)\Gamma^2(p/2+1)-\Gamma(p+1)}{\Gamma(p+1)-\Gamma^2(p/2+1)},\\&\beta|H_0=\tfrac{N\Gamma(p/2+1)}{\Gamma(p+1)-\Gamma^2(p/2+1)},\\&\beta|H_1=A_H^{p/2}\cdot\beta|H_0.\end{aligned}$$

Since $\alpha|H_0=\alpha|H_1$, we simply denote them by α. Thus, the probability of T exceeding λ under hypotheses H can be expressed as the CCDF of (16) as

$$\mathbb{P}^{\text{Lag}}(T>\lambda|H)=1-\sum_{n=0}^{N_g}\frac{r_n|H\cdot\beta|H}{\Gamma(\alpha+1)}\sum_{u=0}^{n}\zeta(u,n,\alpha,\lambda), \tag{17}$$

where $r_n|H$ for each $H\in\{H_1,H_0\}$ is obtained from (14) by replacing α, $\beta|H_1$ and $\beta|H_0$ for hypothesis H_1 and H_0, respectively. Hence, the resulting expressions under H_1 and H_0 yield the desired detection probability P_d^{Lag} and false alarm probability P_f^{Lag}, respectively.

Note that (17) is obtained by approximating the PDF of T by a weighted sum of a finite number (N_g) of identically distributed Gamma random variables whose weights depend on the corresponding Laguerre-polynomials. Interestingly, our numerical results in Section V reveal that the Laguerre approximation is more versatile than the Gamma approximation and more accurate than the CLT approximation (for a few samples).

IV. Analysis in Fading and Diversity Combining

In this section, a unified approach based on the series-MGF obtained in Section III-B is developed for deriving the average detection probability in various fading and diversity reception scenarios. Specifically, average detection probabilities over the κ-μ and the α-μ fading are derived. As well, for a multiple-antenna p-norm detector, the performance of the two proposed

[6] In this paper, the usefulness of the Laguerre approximation is demonstrated by using only a few summands N_g. For a detailed convergence analysis of the approach, we refer the readers to [35]–[37].

[7] Note that the factor β in the denominator outside the summation in (14) necessary to normalize the area under the PDF (13) to unity is missing in [24, eq. (10)].

[8] The superscript 'Lag' is used as shorthand notation for 'Laguerre'.

This article has been accepted for publication in a future issue of this journal, but has not been fully edited. Content may change prior to final publication. Citation information: DOI 10.1109/TVT.2014.2298395, IEEE Transactions on Vehicular Technology

schemes, the pLC and the pLS, and of the classical MRC and SC schemes are derived in Nakagami-m fading channels.

For fading channels, the instantaneous received SNRs $\gamma_i = |h_i|^2\sigma_S^2/\sigma_w^2$, $\forall i \in \{1,2,...,N\}$ are random variables whose PDFs depend on the fading channel (and/or diversity-combining) model. Then, the probability of detection would depend on the instantaneous SNRs $\boldsymbol{\gamma} = \{\gamma_1,\gamma_2,...,\gamma_N\}$. Hence, the average probability of detection $\overline{P}_d$ must be obtained by integrating the instantaneous probability of detection $P_d(\boldsymbol{\gamma})$ over the joint PDF (JPDF) $f(\boldsymbol{\gamma})$. Using (3) and (6), $P_d(\boldsymbol{\gamma})$ can be expressed as

$$P_d(\boldsymbol{\gamma}) = 1 - \frac{1}{2\pi\jmath}\int_B \frac{\mathcal{M}_{T|H_1}(s,\boldsymbol{\gamma})}{s}\, e^{s\lambda} ds, \qquad (18)$$

where $\mathcal{M}_{T|H_1}(s,\boldsymbol{\gamma})$ is the MGF of $T|H_1$ conditioned on $\boldsymbol{\gamma}$. Then, $\overline{P}_d$ can be obtained by integrating (18) over the JPDF $f(\boldsymbol{\gamma})$ as

$$\overline{P}_d = 1 - \frac{1}{2\pi\jmath}\int_{\boldsymbol{\gamma}}\int_B \frac{\mathcal{M}_{T|H_1}(s,\boldsymbol{\gamma})}{s}\, e^{s\lambda} f(\boldsymbol{\gamma}) ds d\boldsymbol{\gamma}. \qquad (19)$$

Interchanging the order of integrations, (19) can be written as

$$\overline{P}_d = 1 - \frac{1}{2\pi\jmath}\int_B e^{s\lambda}\frac{\overline{\mathcal{M}}_{T|H_1}(s)}{s} ds, \qquad (20)$$

where $\overline{\mathcal{M}}_{T|H_1}(s) = \int_{\boldsymbol{\gamma}} \mathcal{M}_{T|H_1}(s,\boldsymbol{\gamma}) f(\boldsymbol{\gamma}) d\boldsymbol{\gamma}$ is the unconditional[9] MGF of $T|H_1$. Thus, (20) suggests that the average detection probability can be easily obtained once we have the inverse Laplace transform of the unconditional MGF of $T|H_1$.

To evaluate (20), first, the need is to find $\overline{\mathcal{M}}_{T|H_1}(s)$. For independently faded samples, the JPDF $f(\boldsymbol{\gamma})$ can be expressed as the product of each individual PDFs $f(\gamma_i)$, $\forall i \in \{1,2,...,N\}$. Thus, we have $\overline{\mathcal{M}}_{T|H_1}(s) = \prod_{i=1}^{N} \overline{\mathcal{M}}_{Y_i^p/N|H_1}(s)$, in which $\overline{\mathcal{M}}_{Y_i^p/N|H_1}(s)$ is the unconditional MGF of Y_i^p/N under H_1 given as $\overline{\mathcal{M}}_{Y_i^p/N|H_1}(s) = \int_0^\infty \mathcal{M}_{Y_i^p/N|H_1}(s,\gamma_i) f(\gamma_i) d\gamma_i$ with $f(\gamma_i)$ being the marginal PDF of the instantaneous SNR of the i-th sample and $\mathcal{M}_{Y_i^p/N|H_1}(s,\gamma_i)$ being the conditional (on γ_i) MGF of Y_i^p/N under H_1. Here $\mathcal{M}_{Y_i^p/N|H_1}(s,\gamma_i)$ can be expressed in a series-form following the steps similar to those used in the derivation of (10) after replacing $A_H = 1/(1+\gamma_i)$ as

$$\mathcal{M}_{Y_i^p/N|H_1}(s,\gamma_i) = \frac{2}{p}\sum_{v=0}^{\infty} \frac{(-1)^v N^{2(v+1)/p}}{v!\;\; s^{2(v+1)/p}} \frac{\Gamma\left(\frac{2(v+1)}{p}\right)}{(1+\gamma_i)^{v+1}}. \qquad (21)$$

Thus, for i.i.d. fading, we can write $\overline{\mathcal{M}}_{T|H_1}(s) = [\overline{\mathcal{M}}_{Y_i^p/N|H_1}(s)]^N$. Then, the only need is to obtain $\overline{\mathcal{M}}_{Y_i^p/N|H_1}(s)$. As we will consider various statistical models for $f(\gamma_i)$, we rewrite the unconditional MGF $\overline{\mathcal{M}}_{Y_i^p/N|H_1}(s)$, with the abuse of notations as

$$\overline{\mathcal{M}}^{\text{fd}}_{Y_i^p/N|H_1}(s) = \int_0^\infty \mathcal{M}_{Y_i^p/N|H_1}(s,\gamma)\, f_{\text{fd}}(\gamma) d\gamma, \qquad (22)$$

where the script 'fd' denotes the corresponding fading (and/or diversity-combining) model under consideration. Solution of (22) would subsequently yield $\overline{\mathcal{M}}^{\text{fd}}_{T|H_1}(s)$ and then the application of inverse Laplace transformation on $\overline{\mathcal{M}}^{\text{fd}}_{T|H_1}(s)/s$ (similarly to the application in Section III-B) yields the average probability of detection $\overline{P}_{d,\text{fd}}$ for the corresponding fading (and/or diversity combining) scenario. In the following sections, the unconditional MGF (22) is derived for different channel models and various diversity-combining schemes on a case-by-case basis.

[9]Henceforth, the term "unconditional" implies averaging (integration) over the JPDF $f(\boldsymbol{\gamma})$.

A. The κ-μ Fading-No Diversity

The κ-μ distribution can model a wide variety of fading environments with LOS propagation. The PDF of the instantaneous SNR for this fading model is given by [39]

$$f_{\kappa\text{-}\mu}(\gamma) = \frac{\mu(1+\kappa)^{\frac{\mu+1}{2}} e^{-\mu\kappa}\gamma^{\frac{\mu-1}{2}}}{\kappa^{\frac{\mu-1}{2}}\overline{\gamma}^{\frac{\mu+1}{2}} e^{-\frac{\mu(1+\kappa)}{\overline{\gamma}}\gamma}} I_{\mu-1}\left(2\mu\sqrt{\frac{\kappa(1+\kappa)\gamma}{\overline{\gamma}}}\right), \qquad (23)$$

where $I_\nu(\cdot)$ is the ν-th order modified Bessel function of first kind [34], $\gamma \geq 0$, and $\overline{\gamma}$ is the average received SNR. The parameter $\kappa > 0$ is the ratio of the total power of the dominant components to that of the scattered waves, and

$$\mu = \frac{\mathbb{E}^2\{\gamma\}}{\text{Var}\{\gamma\}}\left(1 + \frac{2\kappa}{(1+\kappa)^2}\right)$$

represents the number of multipath clusters. By replacing the modified Bessel function of first kind in (23) with its infinite series representation [34, eq. (9.6.10)], substituting the resulting series for $f_{\kappa\text{-}\mu}(\gamma)$ into (22), interchanging the order of integration and summation, and finally, using the definition of the confluent hypergeometric function of the second kind [40],

$$U(a,b,z) = \frac{1}{\Gamma(a)}\int_0^\infty e^{-zt} t^{a-1}(1+t)^{b-a-1} dt, \quad a,\, z > 0, \qquad (24)$$

to solve the resulting integral, the unconditional MGF over κ-μ fading $\overline{\mathcal{M}}^{\kappa\text{-}\mu}_{Y_i^p/N|H_1}(s)$ can be derived to be

$$\overline{\mathcal{M}}^{\kappa\text{-}\mu}_{Y_i^p/N|H_1}(s) = \frac{2\,\mu^\mu(1+\kappa)^\mu}{p\, e^{\kappa\mu}\,\overline{\gamma}^\mu} \times \sum_{v=0}^{\infty}\left[\frac{(-1)^v}{v!}\Gamma\left(\frac{2(v+1)}{p}\right)\left(\frac{N}{s}\right)^{\frac{2(v+1)}{p}} \times \sum_{j=0}^{\infty}\frac{\mu^{2j}\kappa^j(1+\kappa)^j}{\overline{\gamma}^j\, j!} U\left(\mu+j, \mu+j-v, \frac{\mu(1+\kappa)}{\overline{\gamma}}\right)\right]. \qquad (25)$$

The expression (25) is utilized to obtain the unconditional MGF of $T|H_1$ over κ-μ fading and subsequently used to deduce the expression for the average detection probability $\overline{P}_{d,\kappa\text{-}\mu}$ in Section IV-D. Truncation of the resulting infinite series occurring in $\overline{P}_{d,\kappa\text{-}\mu}$ is discussed in Section IV-E.

Note that if the η-μ fading model [18] (which is a generalized fading model for non-LOS conditions) is considered, the unconditional MGF similar to (25) can be obtained. Further, the subsequent analysis would be similar and is thus omitted for brevity.

This article has been accepted for publication in a future issue of this journal, but has not been fully edited. Content may change prior to final publication. Citation information: DOI 10.1109/TVT.2014.2298395, IEEE Transactions on Vehicular Technology

B. The α-μ Fading-No Diversity

In α-μ distribution, parameter $\alpha > 0$ models the non-linearity of the propagation medium, and parameter $\mu > 0$ denotes the number of multipath clusters. The PDF of the instantaneous SNR under this fading model is given by [41]

$$f_{\alpha\text{-}\mu}(\gamma) = \frac{\alpha\mu^{\mu}}{2\Gamma(\mu)\tilde{\gamma}^{\alpha\mu/2}}\gamma^{\alpha\mu/2-1}e^{-\mu\left(\frac{\gamma}{\tilde{\gamma}}\right)^{\alpha/2}}, \qquad (26)$$

where $\gamma \geq 0$, and

$$\tilde{\gamma} = \frac{\mu^{2/\alpha}\Gamma(\mu)}{\Gamma(\mu+2/\alpha)}\frac{E_b}{N_0},$$

in which E_b/N_0 is the energy per bit to noise power spectral density ratio. Substituting the PDF (26) into (22) gives

$$\overline{\mathcal{M}}^{\alpha\text{-}\mu}_{Y_i^p/N|H_1}(s) = \frac{2}{p}\sum_{v=0}^{\infty}\Bigg[\frac{(-1)^v}{v!}\Gamma\left(\frac{2(v+1)}{p}\right)\left(\frac{N}{s}\right)^{\frac{2(v+1)}{p}} \times \frac{1}{\Gamma(\mu)}\int_0^{\infty}\frac{\alpha\mu^{\mu}}{2\tilde{\gamma}^{\alpha\mu/2}}\frac{\gamma^{\alpha\mu/2-1}e^{-\mu\left(\frac{\gamma}{\tilde{\gamma}}\right)^{\frac{\alpha}{2}}}}{(1+\gamma)^{v+1}}d\gamma\Bigg]. \qquad (27)$$

Unfortunately, an exact closed-form solution for the integral in (27) appears to be intractable. However, by substituting

$$t = \frac{\mu}{\tilde{\gamma}^{\alpha/2}}\gamma^{\alpha/2},$$

the integral can be alternatively expressed as $\mathcal{I} = \int_0^{\infty} g(t)e^{-t}dt$ with

$$g(t) = t^{\mu-1}\left[1+\frac{t^{2/\alpha}}{\mu^{2/\alpha}\tilde{\gamma}}\right]^{-v-1}.$$

The integral $\mathcal{I}$ can then be approximated by a Gaussian-Laguerre quadrature sum of the form

$$\mathcal{I} = \int_0^{\infty} g(t)e^{-t}dt \approx \sum_{q=1}^{N_Q} w_q g(t_q),$$

where t_q and w_q are the abscissas and weight factors for the Gaussian-Laguerre quadrature integration [34, eq. (25.4.45)]. Thus, (27) can be evaluated as

$$\overline{\mathcal{M}}^{\alpha\text{-}\mu}_{Y_i^p/N|H_1}(s) \approx \frac{2/p}{\Gamma(\mu)}\sum_{v=0}^{\infty}\Bigg[\frac{(-1)^v}{v!}\Gamma\left(\frac{2(v+1)}{p}\right) \times \left(\frac{N}{s}\right)^{\frac{2(v+1)}{p}}\sum_{q=1}^{N_Q} w_q g(t_q)\Bigg]. \qquad (28)$$

The unconditional MGF (28) provides the basis for obtaining the average detection probability $\overline{P_d}_{,\alpha\text{-}\mu}$ in Section IV-D. As (28) is derived using Gaussian-Laguerre approximation for the integral in (27), the accuracy of the approximation is discussed in conjunction with the expression for $\overline{P_d}_{,\alpha\text{-}\mu}$ in Section IV-E.

C. Analysis for Antenna Diversity

In this section, the input to the p-norm detector comprises of a total of L antennas. Two non-coherent combining techniques, pLC and pLS, are proposed and compared against traditional MRC and SC. Note that the proposed schemes can be readily analyzed for κ-μ and α-μ channels. However, as the SNR of the MRC output is given by the sum of the individual branch SNRs (see Section IV-C3), its analysis in κ-μ or α-μ channel requires an exact PDF of the sum of such variates. Such PDFs are not available in the literature.[10] As we are interested in analyzing the effect of diversity-combining on the p-norm detection performance and in determining the performance of pLC and pLS relative to classical MRC and SC, i.i.d. Nakagami-m fading over the diversity branches is considered for further analysis. Each of the diversity-combining scheme is treated separately in the following.

1) p-Law Combining (pLC): A schematic diagram of the proposed pLC scheme is shown in Fig. 1 above. The received signal at each branch is input to its *p-norm device*, which raises each sample to the p-th power followed by sample-averaging. This yields a total of L independent decision variables $T_1, T_2, ..., T_L$, which are added together to obtain the pLC decision variable

$$T_{\text{plc}} = \sum_{l=1}^{L} T_l = \frac{1}{N}\sum_{l=1}^{L}\sum_{i=1}^{N}(Y_{i,l})^p,$$

where $Y_{i,l}$ is the i-th normalized sample received at the l-th branch (this definition is similar to the definition of Y_i in (2) for a single branch).[11] The final decision is made after comparing T_{plc} against the threshold.

The PDF of the received SNR over a single branch Nakagami-m fading is given by [20]

$$f_{\text{Nak}}(\gamma) = \frac{1}{\Gamma(m)}\left(\frac{m}{\overline{\gamma}}\right)^m \gamma^{m-1}e^{-\frac{m}{\overline{\gamma}}\gamma}, \ \ \gamma \geq 0. \qquad (29)$$

We define $\overline{\mathcal{M}}^{\text{plc}}_{(Y_{i,l})^p/N|H_1}(s)$ as the unconditional MGF of $(Y_{i,l})^p/N|H_1$, which can be obtained by substituting (29) into (22) and using the definition of the confluent hypergeometric function of the second kind (24) to solve the resulting integral as

$$\overline{\mathcal{M}}^{\text{plc}}_{(Y_{i,l})^p/N|H_1}(s) = \frac{2}{p}\left(\frac{m}{\overline{\gamma}}\right)^m \times \sum_{v=0}^{\infty}\frac{(-1)^v}{v!}\Gamma\left(\frac{2(v+1)}{p}\right)\left(\frac{N}{s}\right)^{\frac{2(v+1)}{p}} U\left(m, m-v, \frac{m}{\overline{\gamma}}\right). \qquad (30)$$

As $(Y_{i,l})^p/N$ are i.i.d. for all samples $i \in \{1,2,...,N\}$ and for all branches $l \in \{1,2,...,L\}$, the unconditional MGF of the decision variable T_{plc} under H_1 can be expressed as a product of the unconditional MGFs $\overline{\mathcal{M}}^{\text{plc}}_{(Y_{i,l})^p/N|H_1}(s)$ such that $\overline{\mathcal{M}}_{T_{\text{plc}}|H_1} = [\overline{\mathcal{M}}^{\text{plc}}_{(Y_{i,l})^p/N|H_1}(s)]^{NL}$. Note that the MGF

[10] Although approximations of the sum distributions of κ-μ and α-μ variates are available, respectively, in [42] and [43], they require moment matching for estimating the relevant parameters and are beyond the scope of this work.

[11] This scheme may be considered as a generalization of square-law combining (SLC) scheme used in the conventional ED [10].

This article has been accepted for publication in a future issue of this journal, but has not been fully edited. Content may change prior to final publication. Citation information: DOI 10.1109/TVT.2014.2298395, IEEE Transactions on Vehicular Technology

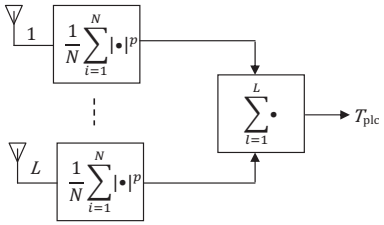

Fig. 1: The proposed p-law combining (pLC) scheme

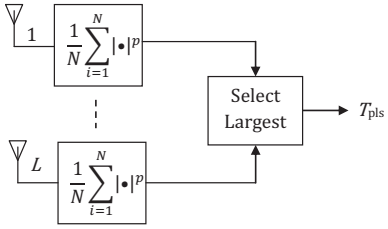

Fig. 2: The proposed p-law selection (pLS) scheme

of T_{plc} under H_0 is $\mathcal{M}_{T_{\text{plc}}|H_0}(s) = [\mathcal{M}_{T|H_0}(s)]^L$, where $\mathcal{M}_{T|H_0}(s)$ is given by (10) with $A_H = 1$. These MGFs form the basis for obtaining the average detection probability $\overline{P_d}_{,\text{plc}}$ and the false alarm probability $P_{f,\text{plc}}$, respectively, in Section IV-D.

2) p-Law Selection (pLS): The proposed pLS scheme is shown in Fig. 2. In this scheme, the received signal at each branch is passed through its p-norm device to obtain L decision variables $T_1, T_2, ..., T_L$. Then, only the branch with the largest decision variable is selected such that the pLS decision variable is given by $T_{\text{pls}} = \max\{T_1, T_2, ..., T_L\}$.[12] The final decision is made after comparing T_{pls} against the threshold. For the independent decision variables, the CDF of T_{pls} can be expressed as

$$\begin{aligned} F_{T,\text{pls}} = \mathbb{P}(T_{\text{pls}} \leq \lambda) &= \mathbb{P}(T_1 \leq \lambda, T_2 \leq \lambda, ..., T_L \leq \lambda) \\ &= \prod_{l=1}^{L}[1 - \mathbb{P}(T_l > \lambda)]. \end{aligned} \tag{31}$$

Since the branches are i.i.d., the false alarm probability of the pLS scheme can be expressed as

$$P_{f,\text{pls}} = 1 - [1 - P_f]^L, \tag{32}$$

where the P_f occurring in (32) is given by (12) for $H = H_0$. Similarly, it is easy to show that the average detection probability for the pLS scheme over Nakagami-m fading channels can be obtained as

$$\overline{P_d}_{,\text{pls}} = 1 - [1 - \overline{P_d}_{,\text{Nak}}]^L, \tag{33}$$

where $\overline{P_d}_{,\text{Nak}}$ is the average detection probability of a single-branch p-norm detector over Nakagami-m fading. Thus, to evaluate (33), only $\overline{P_d}_{,\text{Nak}}$ is needed, which can be obtained from the unconditional MGF (30). The derivation of $\overline{P_d}_{,\text{Nak}}$ is discussed in IV-D.

[12]This scheme may be thought of as generalization of the square-law selection (SLS) scheme used in the ED [10].

3) Maximal Ratio Combining (MRC): MRC is a coherent combining scheme that requires the complete CSI at the receiver [20]. Although the p-norm detector can function without any CSI, the analysis in MRC is important mainly because of its optimality, which helps to establish an upper bound on the achievable detection performance against which other combining schemes may be compared. In MRC, each of the branches is weighted with the complex conjugate of the corresponding fading coefficient and combined to yield the signal $y_{\text{mrc}}(t) = \sum_{l=1}^{L} h_l^* y_l(t)$ where h_l^* and $y_l(t)$ denote the complex conjugate fading coefficient and the received signal respectively, for the l-th branch. The samples of $y_{\text{mrc}}(t)$ are then fed into the p-norm detector.

For a total of L antennas, the MRC output SNR is given by $\gamma^{\text{mrc}} = \sum_{l=0}^{L} \gamma_l$, where γ_l is the SNR of the l-th branch. For i.i.d. branches in Nakagami-m fading, the MRC output SNR is [20]

$$f_{\text{mrc}}(\gamma) = \frac{1}{\Gamma(Lm)}\left(\frac{m}{\overline{\gamma}}\right)^{Lm} \gamma^{Lm-1} e^{-\frac{m}{\overline{\gamma}}\gamma}, \ \ \gamma \geq 0. \tag{34}$$

Then, the unconditional MGF of the i-th sample of the combined signal, Y_i^p/N (with the abuse of notation), can be obtained by substituting (34) into (22) as

$$\begin{aligned} \overline{\mathcal{M}}^{\text{mrc}}_{Y_i^p/N|H_1}(s) = \frac{2}{p}\left(\frac{m}{\overline{\gamma}}\right)^{Lm} \sum_{v=0}^{\infty}\Bigg[\frac{(-1)^v}{v!}\Gamma\left(\frac{2(v+1)}{p}\right) \\ \times \left(\frac{N}{s}\right)^{\frac{2(v+1)}{p}} U\left(Lm, Lm-v, \frac{m}{\overline{\gamma}}\right)\Bigg], \end{aligned} \tag{35}$$

where the definition of the confluent hypergeometric function of second kind (24) is used to solve the resulting integral. The unconditional MGF of $T|H_1$ is then obtained as $\overline{\mathcal{M}}^{\text{mrc}}_{T|H_1}(s) = [\overline{\mathcal{M}}^{\text{mrc}}_{Y_i^p/N|H_1}(s)]^N$, which will be used to derive the corresponding average detection probability $\overline{P_d}_{,\text{mrc}}$ in Section IV-D.

4) Selection Combining (SC): In SC, the branch with the largest SNR is selected so that the resulting SNR is given by $\gamma^{\text{sc}} = \max\{\gamma_1, \gamma_2 ..., \gamma_L\}$. So, the SC is a reduced complexity scheme which processes a single branch and thus, unlike MRC, does not require a coherent sum of all branches' signals [20].

The PDF of output SNR for an SC receiver in i.i.d. Nakagami-m fading channels with integer m is given by [44]

$$\begin{aligned} f_{\text{sc}}(\gamma) = \frac{L}{\Gamma(m)}\sum_{l=0}^{L-1}\Bigg[(-1)^l\binom{L-1}{l}e^{-\frac{(l+1)m}{\overline{\gamma}}\gamma} \\ \times \sum_{\nu=0}^{l(m-1)} \mathcal{B}(\nu, l, m)\left(\frac{m}{\overline{\gamma}}\right)^{m+\nu}\gamma^{m+\nu-1}\Bigg] \end{aligned} \tag{36}$$

for $\gamma \geq 0$, where $\mathcal{B}(\nu, l, m)$ is defined as

$$\mathcal{B}(\nu, l, m) = \sum_{\imath=\nu-m+1}^{\nu} \frac{\mathcal{B}(\imath, l-1, m)}{(\nu-\imath)!} I_{[0,(l-1)(m-1)]}(\imath),$$

with $\mathcal{B}(0, 0, m) = \mathcal{B}(0, l, m) = 1$, $\mathcal{B}(\nu, 1, m) = 1/(\nu!)$, $\mathcal{B}(1, l, m) = l$, and

$$I_{[a,b]}(\imath) = \begin{cases} 1 & a \leq \imath \leq b, \\ 0 & \text{otherwise.} \end{cases}$$

This article has been accepted for publication in a future issue of this journal, but has not been fully edited. Content may change prior to final publication. Citation information: DOI 10.1109/TVT.2014.2298395, IEEE Transactions on Vehicular Technology

By substituting (36) into (22) and then using (24) to solve the resulting integral, the unconditional MGF of Y_i^p/N can be expressed in the form

$$\overline{\mathcal{M}}^{\text{sc}}_{Y_i^p/N|H_1}(s) = \frac{2L}{p\Gamma(m)} \sum_{v=0}^{\infty} \Bigg[\frac{(-1)^v}{v!} \Gamma\left(\frac{2(v+1)}{p}\right) \times \left(\frac{N}{s}\right)^{\frac{2(v+1)}{p}} \sum_{l=0}^{L-1} (-1)^l \binom{L-1}{l} \sum_{\nu=0}^{l(m-1)} \rho(m, \overline{\gamma}, l, v, \nu) \Bigg], \tag{37}$$

where $\rho(m, \overline{\gamma}, l, v, \nu)$ is defined as

$$\rho(m, \overline{\gamma}, L, v, \nu) \triangleq \mathcal{B}(\nu, l, m) \left(\frac{m}{\overline{\gamma}}\right)^{m+\nu} \Gamma(m+\nu) \times U\left(m+\nu, m+\nu-v, \frac{(l+1)m}{\overline{\gamma}}\right).$$

Similar to MRC, the unconditional MGF of $T|H_1$ is then given by $\mathcal{M}^{\text{sc}}_{T|H_1}(s) = [\mathcal{M}^{\text{sc}}_{Y_i^p/N|H_1}(s)]^N$, which will be used to derive the corresponding average detection probability $\overline{P_d}_{,\text{sc}}$ in Section IV-D.

D. Unified Expression for Average Detection Probability Over Fading and Diversity Cases

The derived unconditional MGFs of the decision variables for the respective cases can be expressed in a series-form similar to (11) after using [32, eq. (0.314)]. We denote this form by $\mathcal{M}^{\text{fd}}_{T|H_1}(s)$. Then, by applying the inverse Laplace transform on $\mathcal{M}^{\text{fd}}_{T|H_1}(s)/s$ as in Section III-B, the average detection probability for each of the fading and diversity-combining cases, $\overline{P_d}_{,\text{fd}}$, can be expressed in a single compact form as

$$\overline{P_d}_{,\text{fd}} = 1 - \frac{2^N \xi_{\text{fd}}}{p^N} \sum_{v=0}^{\infty} \frac{C_{v,\text{fd}} \cdot (N\lambda)^{2(v+N)/p}}{\Gamma\left(\frac{2(v+N)}{p}\right)}, \tag{38}$$

with

$$C_{v,\text{fd}} = \frac{1}{v\,\Gamma(2/p) a_{0,\text{fd}}} \sum_{u=1}^{v} (uN - v + u) \frac{(-1)^u}{u!} \times \Gamma\left(\frac{2(u+1)}{p}\right) a_{u,\text{fd}} C_{v-u,\text{fd}}, \quad u \geq 1,$$

and $C_{0,\text{fd}} = [\Gamma(2/p) a_{0,\text{fd}}]^N$. The coefficients $a_{u,\text{fd}}$ appearing in the expression of $C_{v,\text{fd}}$ are dependent on the respective fading and diversity-combining cases and are derived to be

$$a_{u,\kappa\text{-}\mu} = \sum_{j=0}^{\infty} \frac{\mu^{2j} \kappa^j (1+\kappa)^j}{\overline{\gamma}^j j!} U\left(\mu+j, \mu+j-u, \frac{\mu(1+\kappa)}{\overline{\gamma}}\right),$$

$$a_{u,\alpha\text{-}\mu} = \sum_{q=1}^{N_Q} w_q g(t_q), \quad a_{u,\text{mrc}} = U\left(Lm, Lm-u, \frac{m}{\overline{\gamma}}\right),$$

$$a_{u,\text{sc}} = \sum_{l=0}^{L-1} (-1)^l \binom{L-1}{l} \sum_{\nu=0}^{l(m-1)} \rho(m, \overline{\gamma}, l, v, \nu), \tag{39}$$

TABLE III: Number of terms in (38) for computing $\overline{P_d}_{,\kappa\text{-}\mu}$ with 4-decimal points accuracy ($\lambda = 7$).

SNR (dB)	p	N	κ	μ	$V_{\kappa\text{-}\mu}$	J
-15	4.5	6	1.5	2.4	19	15
0	2.7	3	3.2	1.5	25	16
5	1.8	2	4	3.2	36	31
5	3.3	4	1.5	2.2	17	12

TABLE IV: Number of terms in (38) for computing $\overline{P_d}_{,\alpha-\mu}$ with 4-decimal points accuracy.

(SNR (dB), λ)	p	N	α	μ	$V_{\alpha\text{-}\mu}$	N_Q
$(-10, 7)$	4	3	1.5	2.5	18	21
$(-5, 5)$	3	3	1.5	1	23	10
$(3, 5)$	2.5	6	3	2	25	14
$(3, 5)$	1.8	6	2	3.3	74	5

with ξ_{fd} for the corresponding cases defined as

$$\xi_{\kappa\text{-}\mu} \triangleq \left(\frac{\mu(1+\kappa)}{e^{\kappa}\overline{\gamma}}\right)^{N\mu}, \quad \xi_{\alpha\text{-}\mu} \triangleq \left(\frac{1}{\Gamma(\mu)}\right)^N, \quad \xi_{\text{mrc}} \triangleq \left(\frac{m}{\overline{\gamma}}\right)^{NLm}, \quad \xi_{\text{sc}} \triangleq \left(\frac{L}{\Gamma(m)}\right)^N. \tag{40}$$

For the pLC scheme, the average detection probability $\overline{P_d}_{,\text{plc}}$ is given by (38) with $a_{u,\text{plc}} = a_{u,\text{mrc}}|_{L=1}$, and the false alarm probability $P_{f,\text{plc}}$ is given by (12) (for $H = H_0$), with each N occurring in (38) and (12) replaced by NL except the one occurring as $N\lambda$ inside the summation. For the pLS scheme, the average detection probability $\overline{P_d}_{,\text{pls}}$ in (33) requires only $\overline{P_d}_{,\text{Nak}}$, which is given by (38) for MRC with $a_{u,\text{mrc}}|_{L=1}$ and $\xi_{\text{mrc}}|_{L=1}$. For the sake of brevity, we omit re-writing the expressions.

E. Computation of $\overline{P_d}_{,fd}$ in (38)

As is clear from (38) and (39), the final expressions for $\overline{P_d}_{,\text{plc}}$ $\overline{P_d}_{,\text{pls}}$, $\overline{P_d}_{,\text{mrc}}$ and $\overline{P_d}_{,\text{sc}}$ require the evaluation of only a single infinite series-sum similar to that for the AWGN case in (12). The series expression for these cases can then be truncated with a finite number of terms, and the truncation error can be upper bounded in a similar manner.

The expression of $\overline{P_d}_{,\kappa\text{-}\mu}$ contains two infinite series-sums in v and j, which have to be truncated with a finite number of terms for computation. A tight truncation error upper bound for $\overline{P_d}_{,\kappa\text{-}\mu}$ is difficult to obtain due to occurrence of infinite sums in both the numerator and denominator of the recursively computed coefficients $C_{v,\kappa\text{-}\mu}$. Nevertheless, our numerical experiments reveal that the sums are readily converging and can be truncated with a finite number of terms, which can be chosen to achieve the desired precision. For example, the number of terms in v and j (denoted by $V_{\kappa\text{-}\mu}$ and J respectively) for computing $\overline{P_d}_{,\kappa\text{-}\mu}$ with 4-decimal points accuracy are shown in Table III.

Similarly, the expression of $\overline{P_d}_{,\alpha\text{-}\mu}$ requires the evaluation of an infinite series-sum in v and further includes the computation of the Gaussian-Laguerre quadrature sum. Accurate computation of $\overline{P_d}_{,\alpha\text{-}\mu}$ is possible by truncating the infinite series in v with $V_{\alpha\text{-}\mu}$ terms and simultaneously choosing a suitable number of terms N_Q in the quadrature sum to satisfy

This article has been accepted for publication in a future issue of this journal, but has not been fully edited. Content may change prior to final publication. Citation information: DOI 10.1109/TVT.2014.2298395, IEEE Transactions on Vehicular Technology

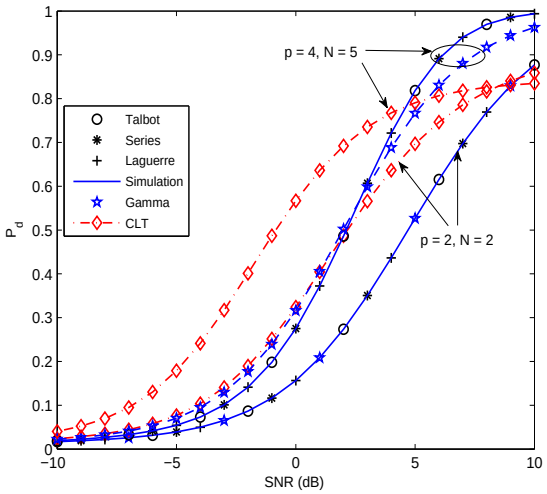

Fig. 3: Comparison of the derived Talbot solution (9), series solution (12) and the Laguerre approximation (17) against the existing Gamma (Appendix I) and CLT (Appendix II) approximations for AWGN.

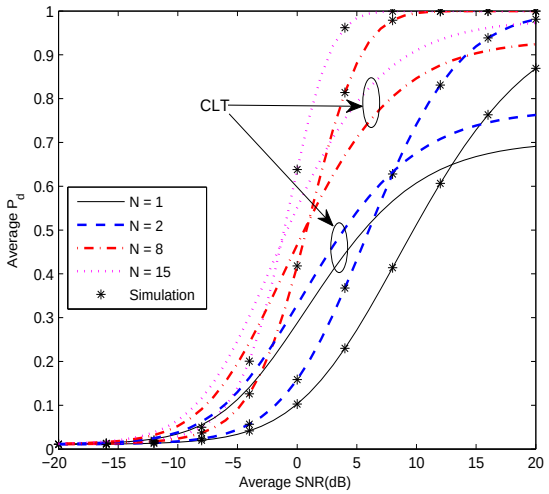

Fig. 4: Average detection probability ($\overline{P_d}$) vs. average SNR ($\overline{\gamma}$) for 3.5-norm detector in Rayleigh fading (using (38) with $\kappa \to 0$, $\mu = 1$) for various samples, compared to the CLT approximation and simulation.

the overall precision requirement. Some examples with various sets of values for 4-decimal points accuracy are shown in Table IV.

V. Numerical Results and Discussions

In this section, the p-norm detector performance is characterized with several P_d vs. SNR curves, and the receiver operating characteristics curves (popularly known as ROC curves), which are the plots of P_d against P_f. Since a low probability of false alarm is highly desirable (e.g., in IEEE 802.22, a CR requires $P_f \leq 0.1$ [45]), we set $P_f = 0.01$ for all of the P_d vs. SNR plots. The detection threshold λ is determined based on this requirement and used for the computation of P_d. On the other hand, the ROC curves are obtained by varying the threshold from a low to a high value (theoretically, from 0 to ∞), and plotting the corresponding P_d against P_f. These curves are important to jointly observe how P_d and P_f vary with the detector parameters (SNR, p, sample size, fading severity, and/or the number of antennas).

A numerical analysis to provide insights into the derived results is presented next. Results of Monte-Carlo simulation performed in MATLAB with 10^6 iterations are included wherever necessary for validating the analysis.

A. Performance in AWGN (Fig. 3)

In Fig. 3, the Talbot method (9), the series solution (12), the Laguerre approximation (17), the Gamma approximation [6] (see Appendix I), and the CLT-based approximation (see Appendix II) are compared. The results plotted for two different combinations of (p, N), namely $(p = 2, N = 2)$ and $(p = 4, N = 5)$, give the following insights:

(i) The Talbot solution (9) and the series-based solution (12) match exactly with the simulation results for both sets of (p, N), thus validating the accuracy (exactness) of these solutions.

(ii) For $p = 2$, the Gamma approximation is exact since the decision variable is then a Gamma-distributed sum of N independent exponential random variables. However, for another p ($p = 4$), the decision variable is no longer Gamma distributed, and the Gamma approximation deviates from the simulation. Interestingly, the proposed Laguerre approximation matches the simulation for both p values.

(iii) The Laguerre approximation has remarkably better accuracy than the CLT approximation.

Hence, from (ii)-(iii), we can say that the Laguerre approximation is more versatile than the Gamma approximation and is more accurate than the CLT approximation (for a few samples).

B. Effect of sample size N (Fig. 4)

The sample size N is a critical performance-determining parameter of the detector. Hence, the effect of N on the detection probability ($\overline{P_d}$) over the Rayleigh fading channel (obtained from $\overline{P}_{d,\kappa\text{-}\mu}$ in (38) with $\kappa \to 0$, $\mu = 1$) is studied in Fig. 4 for a 3.5-norm detector. The CLT approximation is plotted for comparison. The results reveal that

(i) The reliability of detection improves drastically with the number of received signal samples as compared to the reliability of the detector with one sample ($N = 1$) considered in [8] and [9]. For example, at SNR of 10 dB, the 2-samples-based detector ($N = 2$) yields about 45% higher detection probability than the one-sample detector. Furthermore, even at a low SNR of -10 dB, the 15-samples-based detector obtains about an 86% gain in detection probability compared to the single sample-based detector.

(ii) The CLT approximation[13] deviates significantly, although

[13]Obtained by numerically integrating $P_{d,\text{CLT}}$ (see Appendix II) over the Rayleigh fading PDF $f(\gamma) = 1/\overline{\gamma} \cdot \exp(-\gamma/\overline{\gamma})$, $\gamma \geq 0$.

This article has been accepted for publication in a future issue of this journal, but has not been fully edited. Content may change prior to final publication. Citation information: DOI 10.1109/TVT.2014.2298395, IEEE Transactions on Vehicular Technology

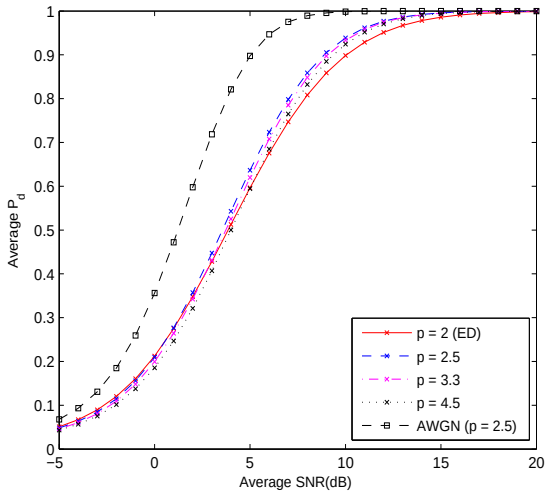

Fig. 5: Average detection probability ($\overline{P_{d,\kappa\text{-}\mu}}$) vs. average SNR ($\overline{\gamma}$) in a $\kappa = 1.5$, $\mu = 2.2$ fading channel for various p with $N = 6$. The AWGN plot is included for comparison. Discrete marks indicate simulation values.

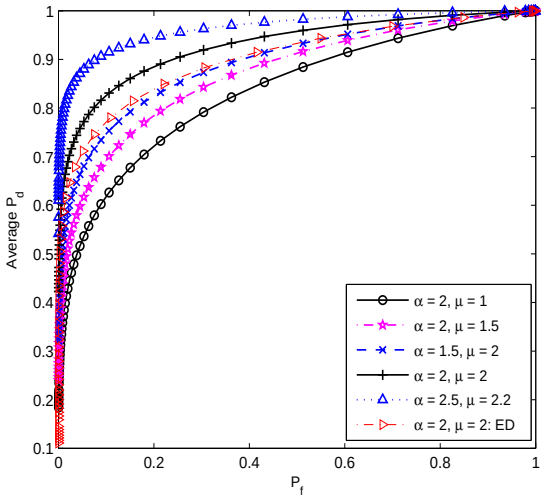

Fig. 7: ROC curves of a 2.7-norm detector for various α-μ channels at SNR $= 3$ dB, $N = 5$. The ED ($p = 2$) plot is included for comparison. The discrete marks on the graphs indicate the simulation results.

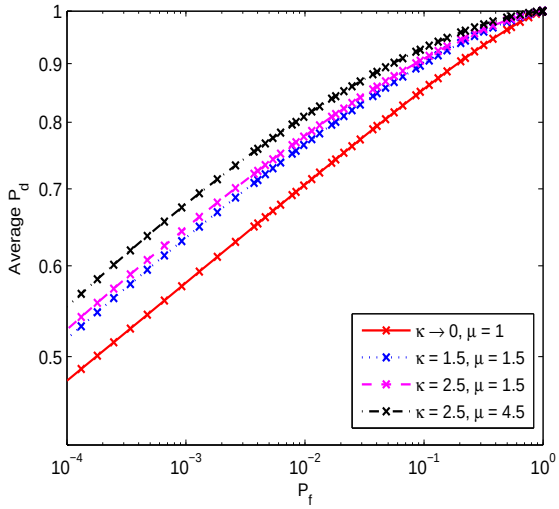

Fig. 6: ROC curves (in log-log scale) for a 3-norm detector with $N = 3$ for various κ-μ channels at SNR of 7 dB. The discrete marks indicate the simulation results.

its accuracy improves with an increase in sample size.

C. Analysis in κ-μ fading (Fig. 5 and Fig. 6)

The effect of p on the detection probability $\overline{P_{d,\kappa\text{-}\mu}}$ in (38) for a fixed LOS ($\kappa = 1.5$) and fixed multipath ($\mu = 2.2$) condition is illustrated in Fig. 5. The following observations are made:

(i) The ED ($p = 2$) does not necessarily yield the best detection performance in κ-μ fading channels compared to other detectors with $p \neq 2$. For example, at SNR of 7 dB with $N = 6$, the 2.5-norm detector achieves 7% higher $\overline{P_{d,\kappa\text{-}\mu}}$ than that of the ED. The 3.3-norm detector is the second-best one, when the SNR exceeds 2 dB. Even the 4.5-norm detector possesses a higher $\overline{P_{d,\kappa\text{-}\mu}}$ than that of the ED for a received SNR above 6 dB. Thus, the ED is not necessarily the best choice among all p in non-homogeneous LOS propagation.

(ii) The comparison with the AWGN (no fading) reveals that multipath fading severely affects the p-norm detection performance. For example, at an SNR of 2 dB, the detection probability reduces by as much as 40% compared to the corresponding case without fading for a 2.5-norm detector.

In Fig. 6, the ROC curves (plotted in log-log scale for clarity) of a 3-norm detector with $N = 3$ for several LOS and multipath conditions are shown. For a fixed multipath effect (fixed μ), the detector performs better at stronger LOS (higher κ) conditions. Likewise, the performance improves with the increased multipath effect (higher μ) for a given LOS strength (fixed κ). These results indicate the advantages of propagation environments having a stronger LOS and a higher number of multipath components on the detection performance.

D. Analysis in α-μ fading (Fig. 7)

The effect of non-linear propagation on the p-norm detection performance ($p = 2.7$) is presented in Fig. 7 for various instances of the α-μ fading channel. Additionally, an ED ($p = 2$) plot and the simulation results are included for comparison. The following observations are made:

(i) The analytical results for $\overline{P_{d,\alpha\text{-}\mu}}$ in (38) and the simulation results match, thus validating the accuracy of the Gaussian-Laguerre quadrature integration used for deriving $\overline{P_{d,\alpha\text{-}\mu}}$.

(ii) The increased non-linearity of the propagation medium (higher α) for a fixed multipath effect (fixed μ) has a positive effect on the detection performance. As well, the performance is better for a larger multipath effect (higher μ) at a given non-linearity (fixed α). For example, at $P_f \approx 0.1$, when α increases from 1.5 to 2 at $\mu = 2$, an

This article has been accepted for publication in a future issue of this journal, but has not been fully edited. Content may change prior to final publication. Citation information: DOI 10.1109/TVT.2014.2298395, IEEE Transactions on Vehicular Technology

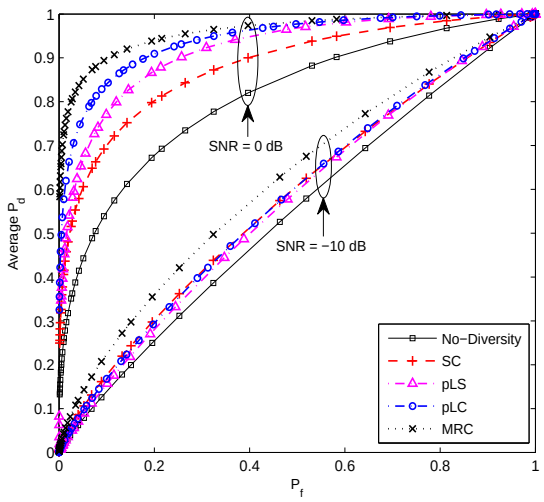

Fig. 8: Two sets of ROC curves at SNR -10 dB ($p = 2.5$, $N = 3$) and 0 dB ($p = 3$, $N = 4$) for various diversity-combining schemes in Nakagami-3 fading channels with $L = 3$. No-diversity curves are included for comparison. The discrete marks on the graphs indicate the simulation results.

approximately 11% gain in $\overline{P_{d,\alpha\text{-}\mu}}$ is obtained. Likewise, about a 20% increase in $\overline{P_{d,\alpha\text{-}\mu}}$ results when μ increases from 1 to 1.5 at $\alpha = 2$.

(iii) The results also suggest that ED ($p = 2$) is not necessarily the best choice (among all p) for detecting signals affected by the non-linearity of the wireless channel. For example, at $P_f \approx 0.1$, over a channel with $\alpha = 2$ and $\mu = 2$, the 2.7-norm detector yields about a 7.5% higher $\overline{P_{d,\alpha\text{-}\mu}}$ than the ED.

E. Analysis with diversity-combining (Fig. 8)

The boost in p-norm detection performance due to antenna diversity is depicted in Fig. 8. Furthermore, to assess the relative performance gains of the pLC, pLS, MRC and SC schemes, they are compared against each other and with the no-diversity (single-antenna) case as well. The following insights are evident:

(i) Antenna diversity boosts the detection performance: Even at a low SNR of -10 dB with $P_f \approx 0.1$, the 2.5-norm detector deploying a 3-branch MRC has about a 53% increase in detection probability compared to the no-diversity case.

(ii) Performance of pLC, pLS, MRC and SC: As expected, MRC has the best performance among all the schemes. Interestingly, the proposed pLC and pLS schemes perform quite similarly to the traditional SC at low SNR (plots at -10 dB), while both of them outperform SC at a relatively high SNR (plots at 0 dB). For instance, at an SNR of 0 dB for $P_f \approx 0.1$, the 3-norm detector ($N = 4$) with SC, pLS, pLC and MRC schemes yields, respectively, about 28%, 40%, 54% and 66% increase in detection probability compared to the no-diversity case. Note that the pLC performs closer (than pLS and SC) to the optimal MRC. As a final note, the MRC relies on the availability of full CSI for each branch while the SC requires constant monitoring of all the branches in order to find the branch with the maximum SNR [20]. However, these requirements lead to higher complexity and cost for practical implementation. Thus, the proposed pLC and pLS schemes may offer better alternatives than the MRC and SC schemes, particularly, for a non-coherent device like the p-norm detector.

VI. Conclusion and Future Work

In this paper, a comprehensive p-norm detector performance analysis for non-fading (AWGN), generalized fading and with several antenna diversity-combining schemes is presented by developing several analytical/numerical solutions for P_d and P_f. To evaluate P_d and P_f for AWGN channels, the MGF of the decision variable is derived in two forms: (i) closed-form for even-integer p, and (ii) series-form for arbitrary p. A numerical method utilizing the Talbot inversion is developed for case (i), and infinite series expansion with convergence acceleration based on the ϵ-algorithm is derived for case (ii). Additionally, a new approximation based on the Laguerre polynomial series is shown to be more versatile compared to the existing Gamma approximation and more accurate than the CLT approximation. To quantify the impact of the fading channels, the series MGF-based analysis is extended to cover the κ-μ and α-μ fading channels, thus helping to quantify the detection performance in more realistic fading environments. To capitalize on antenna diversity, non-coherent pLC and pLS schemes which do not require any CSI are proposed. Their performances along with those of the traditional MRC and SC schemes are derived for Nakagami-m fading. Interestingly, both pLC and pLS perform similar to the SC at low SNR, while outperforming it at relatively high SNR. Further, pLC performs the closest (among all the schemes) to the optimal MRC at higher SNR. Moreover, the proposed pLC and pLS schemes are more suitable than the MRC and SC schemes for the p-norm detector, which can function without any CSI.

Future research directions include fine-tuning p to maximize the detection performance, and investigation of the detection performance of a cooperative network of detectors, each deploying an optimized p-norm detector operating in generic fading environments.

Appendix: Gamma approximation (I) and CLT approximation (II) for AWGN

(I) If we assume the decision variable T to be Gamma distributed, the detection probability ($P_{d,\text{Gam}}$) and false alarm probability ($P_{f,\text{Gam}}$) can be derived on the basis of [6] as $P_{d,\text{Gam}} = 1-\mathcal{G}(\lambda/\theta_1, k_1)/\Gamma(k_1)$ and $P_{f,\text{Gam}} = 1-\mathcal{G}(\lambda/\theta_0, k_0)/\Gamma(k_0)$, where the parameters are given by $k_0 = k_1 = N\Gamma^2(p/2+1)/[\Gamma(p+1)-\Gamma^2(p/2+1)]$, $\theta_0 = [\Gamma(p+1)-\Gamma^2(p/2+1)]/[N\Gamma(p/2+1)]$, and $\theta_1 = (1+\gamma)^{p/2}\theta_0$.

(II) When the number of samples is very large ($N \gg 1$), the CLT may be invoked such that T is Gaussian distributed with mean $\mu_0 = \Gamma(p/2+1)$ and variance $\sigma_0^2 = [\Gamma(p+1)-\Gamma^2(p/2+1)]/N$ under H_0, or with mean $\mu_1 =$

$(1+\gamma)^{p/2}\mu_0$ and variance $\sigma_1^2 = (1+\gamma)^p\sigma_0^2$ under H_1. It is straightforward to show that the CDF of T under both hypotheses can be expressed in terms of the Gaussian-Q function $Q(x) = (1/\sqrt{2\pi})\int_x^\infty e^{-t^2/2}dt$. Then, the detection and false alarm probabilities utilizing the CLT approximation can be easily expressed as

$$P_{d,\text{CLT}} = Q\left(\frac{\lambda-\mu_1}{\sigma_1}\right), \quad P_{f,\text{CLT}} = Q\left(\frac{\lambda-\mu_0}{\sigma_0}\right).$$

REFERENCES

[1] H. L. Van Trees, *Detection, Estimation, and Modulation Theory, Part III, Radar-sonar Signal Processing and Gaussian Signals in Noise*. Wiley, New York, 2001.

[2] D. Cabric, S. Mishra, and R. Brodersen, "Implementation issues in spectrum sensing for cognitive radios," in *Proc. Asilomar Conf. Signals, Systems and Computers*, 2004, pp. 772–776.

[3] E. Arias-de Reyna, A. D'Amico, and U. Mengali, "UWB energy detection receivers with partial channel knowledge," in *Proc. IEEE Int. Conf. Communications (ICC)*, 2006, pp. 4688–4693.

[4] D. Cabric, "Addressing feasibility of cognitive radios," *IEEE Signal Process. Mag.*, vol. 25, no. 6, pp. 85–93, Nov. 2008.

[5] H. Urkowitz, "Energy detection of unknown deterministic signals," *Proc. IEEE*, vol. 55, no. 4, pp. 523–531, Apr. 1967.

[6] Y. Chen, "Improved energy detector for random signals in Gaussian noise," *IEEE Trans. Wireless Commun.*, vol. 9, no. 2, pp. 558–563, Feb. 2010.

[7] F. Moghimi, A. Nasri, and R. Schober, "Adaptive L_p-norm spectrum sensing for cognitive radio networks," *IEEE Trans. Commun.*, vol. 59, no. 7, pp. 1934–1945, July 2011.

[8] A. Singh, M. Bhatnagar, and R. Mallik, "Optimization of cooperative spectrum sensing with an improved energy detector over imperfect reporting channels," in *Proc. IEEE Veh. Technol. Conf. (VTC Fall)*, 2011.

[9] A. Singh, M. R. Bhatnagar, and R. K. Mallik, "Cooperative spectrum sensing in multiple antenna based cognitive radio network using an improved energy detector," *IEEE Commun. Lett.*, vol. 16, no. 1, pp. 64–66, Jan. 2012.

[10] F. Digham, M.-S. Alouini, and M. K. Simon, "On the energy detection of unknown signals over fading channels," *IEEE Trans. Commun.*, vol. 55, no. 1, pp. 21–24, Jan. 2007.

[11] V. Kostylev, "Energy detection of a signal with random amplitude," in *Proc. IEEE Int. Conf. Communications (ICC)*, 2002, pp. 1606–1610.

[12] S. Atapattu, C. Tellambura, and H. Jiang, "Analysis of area under the ROC curve of energy detection," *IEEE Trans. Wireless Commun.*, vol. 9, no. 3, pp. 1216–1225, Mar. 2010.

[13] S. Atapattu, C. Tellambura, and H. Jiang, "Performance of an energy detector over channels with both multipath fading and shadowing," *IEEE Trans. Wireless Commun.*, vol. 9, no. 12, pp. 3662–3670, Dec. 2010.

[14] S. P. Herath, N. Rajatheva, and C. Tellambura, "Energy detection of unknown signals in fading and diversity reception," *IEEE Trans. Commun.*, vol. 59, no. 9, pp. 2443–2453, Sep. 2011.

[15] A. Annamalai, O. Olabiyi, S. Alam, O. Odejide, and D. Vaman, "Unified analysis of energy detection of unknown signals over generalized fading channels," in *Proc. Int. Wireless Commun. and Mobile Computing Conf. (IWCMC)*, 2011, pp. 636–641.

[16] A. Makarfi and K. Hamdi, "Efficiency of energy detection for spectrum sensing in a Poisson field of interferers," in *Proc. IEEE Wireless Communications and Networking Conf. (WCNC)*, 2012, pp. 1023–1028.

[17] P. Sofotasios, E. Rebeiz, L. Zhang, T. Tsiftsis, D. Cabric, and S. Freear, "Energy detection based spectrum sensing over κ-μ and κ-μ extreme fading channels," *IEEE Trans. Veh. Technol.*, vol. 62, no. 3, pp. 1031–1040, Mar. 2013.

[18] M. D. Yacoub, "The $\kappa-\mu$ distribution and the $\eta-\mu$ distribution," *IEEE Antennas Propag. Mag.*, vol. 49, no. 1, pp. 68–81, Feb. 2007.

[19] M. D. Yacoub, "The $\alpha-\mu$ distribution: a physical fading model for the stacy distribution," *IEEE Trans. Veh. Technol.*, vol. 56, no. 1, pp. 27–34, Jan. 2007.

[20] M. K. Simon and M.-S. Alouini, *Digital Communication over Fading Channels*, 2nd ed. New York: Wiley, 2005.

[21] A. Talbot, "The accurate numerical inversion of Laplace transforms," *IMA Journal of Applied Mathematics*, vol. 23, no. 1, pp. 97–120, 1979.

[22] J. Abate and P. P. Valkó, "Multi-precision Laplace transform inversion," *International Journal for Numerical Methods in Engineering*, vol. 60, pp. 979–993, May 2004.

[23] P. Wynn, "On the convergence and stability of the epsilon algorithm," *SIAM Journal on Numerical Analysis*, vol. 3, no. 1, pp. 91–122, Mar. 1966.

[24] H. Mustafa and R. Dimitrakopoulos, "Generalized Laguerre expansions of multivariate probability densities with moments," *ACM Journal of Computer and Mathematics with Applications*, vol. 60, no. 7, pp. 2178–2189, Oct. 2010.

[25] R. Tandra and A. Sahai, "SNR walls for signal detection," *IEEE J. Sel. Areas Commun.*, vol. 2, no. 1, pp. 4–17, 2008.

[26] A. Taherpour, M. Nasiri-Kenari, and S. Gazor, "Multiple antenna spectrum sensing in cognitive radios," *IEEE Trans. Wireless Commun.*, vol. 9, no. 2, pp. 814–823, Feb. 2010.

[27] S. Wei, D. Goeckel, and P. Kelly, "Convergence of the complex envelope of bandlimited OFDM signals," *IEEE Trans. Inf. Theory*, vol. 56, no. 10, pp. 4893–4904, Oct. 2010.

[28] D. Middleton, "On the detection of stochastic signals in additive normal noise–I," *IRE Trans. Inf. Theory*, vol. 3, no. 2, pp. 86–121, June 1957.

[29] G. L. Stuber, *Principles of Mobile Communication*. Kluwer Academic Publishers, New York, 2001.

[30] Z. Liu, X. Ma, and G. Giannakis, "Space-time coding and Kalman filtering for time-selective fading channels," *IEEE Trans. Commun.*, vol. 50, no. 2, pp. 183–186, Feb. 2002.

[31] J. Cheng, C. Tellambura, and N. C. Beaulieu, "Performance of digital modulations on Weibull slow-fading channels," *IEEE Trans. Commun.*, vol. 52, no. 8, pp. 1265–1268, Aug. 2004.

[32] I. S. Gradshteyn and I. Ryzhik, *Tables of Integrals, Series and Products*, 7th ed. London: Academic, 2007.

[33] R. C. Palat, A. Annamalai, and J. H. Reed, "An efficient method for evaluating information outage probability and ergodic capacity of OSTBC system," *IEEE Commun. Lett.*, vol. 12, no. 3, pp. 191–193, Mar. 2004.

[34] M. Abramowitz and I. A. Stegun, *Handbook of Mathematical Functions with Formulas, Graphs and Mathematical Tables*. National Bureau of Standards, Nov. 1970.

[35] E. Hille, "On Laguerre's series: first note," *Proc. Natl. Acad. Sci. USA*, vol. 12, no. 4, pp. 261–265, Apr. 1926.

[36] E. Hille, "On Laguerre's series: second note," *Proc. Natl. Acad. Sci. USA*, vol. 12, no. 4, pp. 265–269, Apr. 1926.

[37] E. Hille, "On Laguerre's series: third note," *Proc. Natl. Acad. Sci. USA*, vol. 12, no. 5, pp. 348–352, May 1926.

[38] Wolfram. [Online]. Available: http://functions.wolfram.com/Polynomials/LaguerreL3/02/

[39] S. Atapattu, C. Tellambura, and H. Jiang, "A mixture gamma distribution to model the SNR of wireless channels," *IEEE Trans. Wireless Commun.*, vol. 10, no. 12, pp. 4193–4203, Dec. 2011.

[40] E. W. Weisstein, "Confluent hypergeometric function of the second kind." [Online]. Available: http://mathworld.wolfram.com/ConfluentHypergeometricFunctionoftheSecondKind.html

[41] A. M. Magableh and M. Matalgah, "Moment generating function of the generalized α-μ distribution with applications," *IEEE Commun. Lett.*, vol. 13, no. 6, pp. 411–413, June 2009.

[42] D. da Costa and M. Yacoub, "Accurate approximations to the sum of generalized random variables and applications in the performance analysis of diversity systems," *IEEE Trans. Commun.*, vol. 57, no. 5, pp. 1271–1274, May 2009.

[43] D. da Costa, M. Yacoub, and J. C. S. S. Filho, "Highly accurate closed-form approximations to the sum of α-μ variates and applications," *IEEE Trans. Wireless Commun.*, vol. 7, no. 9, pp. 3301–3306, Sep. 2008.

[44] A. Annamalai and C. Tellambura, "Performance evaluation of generalized selection diversity systems over Nakagami-m fading channels," *Wireless Commun. Mobile Comput.*, vol. 3, no. 1, pp. 99–116, Feb. 2003.

[45] C. Stevenson, G. Chouinard, Z. Lei, W. Hu, S. Shellhammer, and W. Caldwell, "IEEE 802.22: The first cognitive radio wireless regional area network standard," *IEEE Commun. Mag.*, vol. 47, no. 1, pp. 130–138, Jan. 2009.

Vesh Raj Sharma Banjade received the B.Eng. Degree in Electronics and Communications Engineering from the Institute of Engineering, Pulchowk Campus, Nepal in 2009 and M.Eng. Degree in Telecommunications Engineering from the Asian Institute of Technology (AIT), Thailand in 2011. He is currently working towards the Ph.D. degree in Electrical and Computer Engineering at the University of Alberta, Canada. His research interests include wireless signal detection, spectrum sensing in cognitive radios, and cooperative communications.

Chintha Tellambura (F'11) received the B.Sc. degree (with first-class honor) from the University of Moratuwa, Sri Lanka, in 1986, the M.Sc. degree in Electronics from the University of London, U.K., in 1988, and the Ph.D. degree in Electrical Engineering from the University of Victoria, Canada, in 1993.

He was a Postdoctoral Research Fellow with the University of Victoria (1993-1994) and the University of Bradford (1995-1996). He was with Monash University, Australia, from 1997 to 2002. Presently, he is a Professor with the Department of Electrical and Computer Engineering, University of Alberta. His research interests focus on communication theory dealing with the wireless physical layer.

Prof. Tellambura is an Associate Editor for the IEEE TRANSACTIONS ON COMMUNICATIONS and the Area Editor for Wireless Communications Systems and Theory in the IEEE TRANSACTIONS ON WIRELESS COMMUNICATIONS. He was Chair of the Communication Theory Symposium in Globecom'05 held in St. Louis, MO.

Hai Jiang (M'07) received the B.Sc. and M.Sc. degrees in Electronics Engineering from Peking University, Beijing, China, in 1995 and 1998, respectively, and the Ph.D. degree (with an Outstanding Achievement in Graduate Studies Award) in electrical engineering from the University of Waterloo, Waterloo, Ontario, Canada, in 2006.

Since 2007, he has been a faculty member at the University of Alberta, Edmonton, Alberta, Canada, where he is currently an Associate Professor in the Department of Electrical & Computer Engineering. His research interests include radio resource management, cognitive radio networking, and cross-layer design for wireless multimedia communications.